

Quantitative PET Image Reconstruction

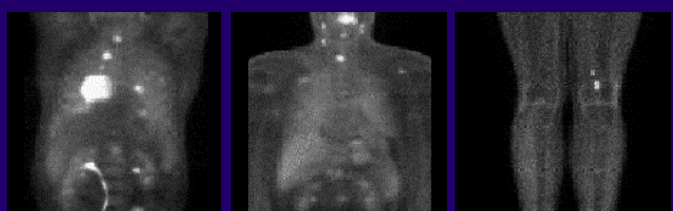
Richard Leahy

Signal and Image Processing Institute, USC

- Why PET?
- 3D Reconstruction
- 4D Reconstruction
- Performance analysis

Glucose Metabolism

- Increased metabolic rate in malignant tumors leads to increased uptake of ^{18}F -Fluorodeoxyglucose (FDG).



Also a marker of metabolism in heart and brain

Positron-Emitting Radionuclides

Isotope	Halflife	β^+ fraction	Max. Energy	range(mm)	production
C-11	20.4 mins	0.99	0.96 MeV	0.4 mm	cyclotron
N-13	9.96 mins	1.00	1.20 MeV	0.7 mm	cyclotron
O-15	123 secs	1.00	1.74 MeV	1.1 mm	cyclotron
F-18	110 mins	0.97	0.63 MeV	0.3 mm	cyclotron
Cu-62	9.74 mins	0.98	2.93 MeV	2.7 mm	generator
Cu-64	12.7 hours	0.19	0.65 MeV	0.3 mm	cyclotron
Ga-68	68.3 mins	0.88	1.83 MeV	1.2 mm	generator
Br-76	16.1 hours	1.00	1.90 MeV	1.2 mm	cyclotron
Rb-82	78 secs	0.96	3.15 MeV	2.8 mm	generator
I-124	4.18 days	0.22	1.50 MeV	0.9 mm	cyclotron

Tracers/Probes

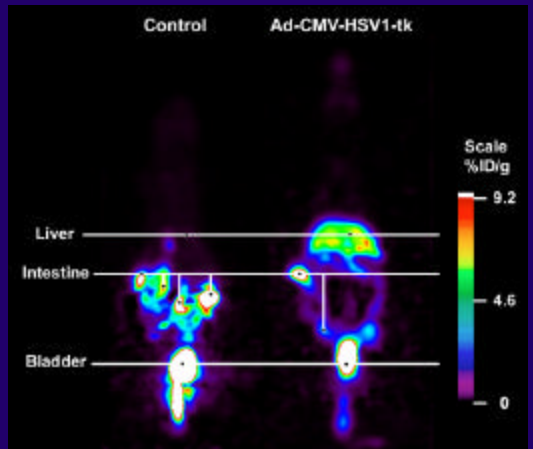
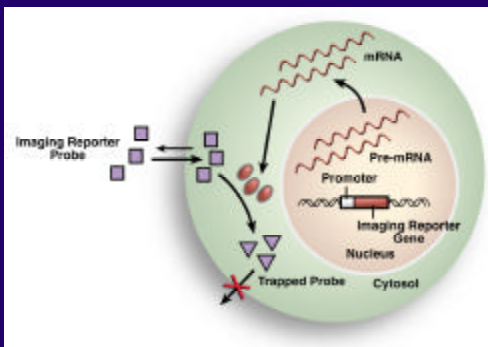


cyclotron
 ^{11}C , ^{13}N , ^{15}O , ^{18}F

hemodynamic parameters (H_2^{15}O , ^{15}O -butanol, ^{11}CO , $^{13}\text{NH}_3$)
 substrate metabolism(^{18}F -FDG, $^{15}\text{O}_2$, ^{11}C -palmitic acid....)
 protein synthesis (^{11}C -leucine, ^{11}C -methionine, ^{11}C -tyrosine)
 enzyme activity (^{11}C -deprendyl, ^{18}F -deoxyuracil...)
 drugs (^{11}C -cocaine, ^{13}N -cisplatin, ^{18}F -fluorouracil...)
 receptor affinity (^{11}C -raclopride, ^{11}C -carfentanil, ^{11}C -scopalamine)
 neurotransmitter biochemistry (^{18}F -fluorodopa, ^{11}C -ephedrine...)
 gene expression (^{18}F -penciclovir, ^{18}F -antisense oligonucleotides...)

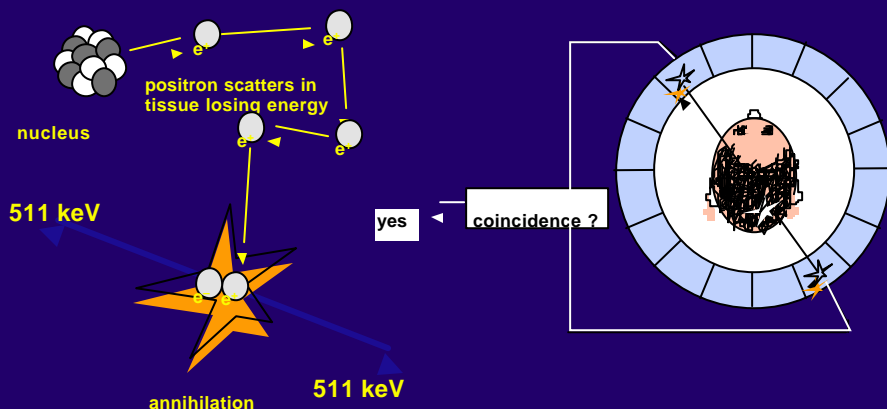
.....

Imaging Gene Expression by PET

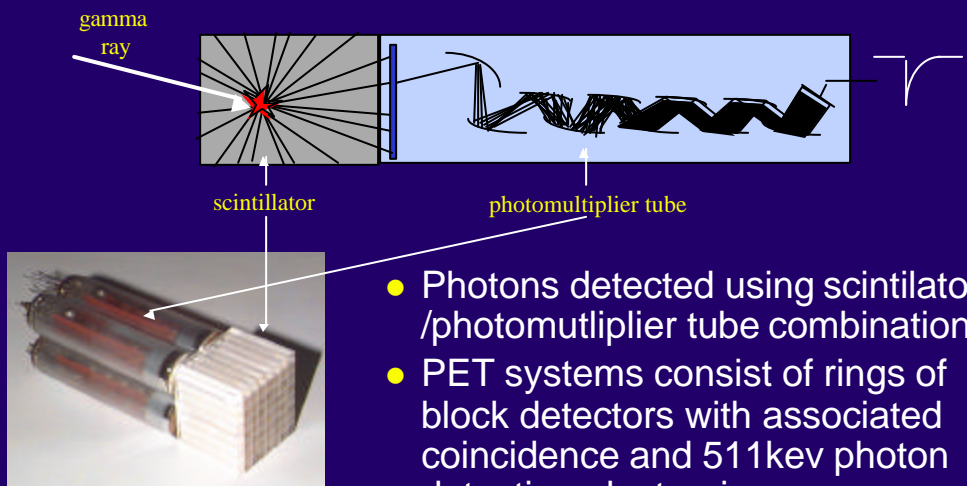


Sam Gambhir, Harvey Herschman, Michael Phelps et al

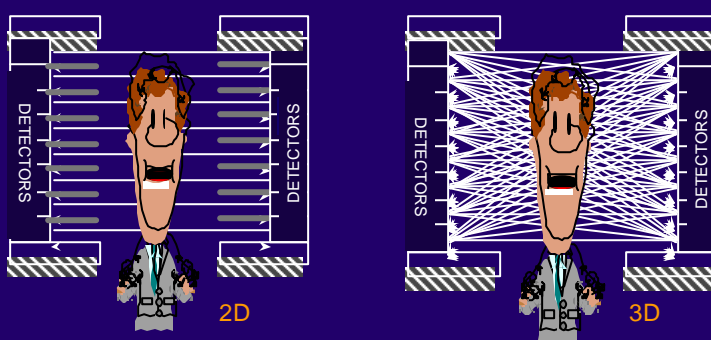
Coincidence Detection



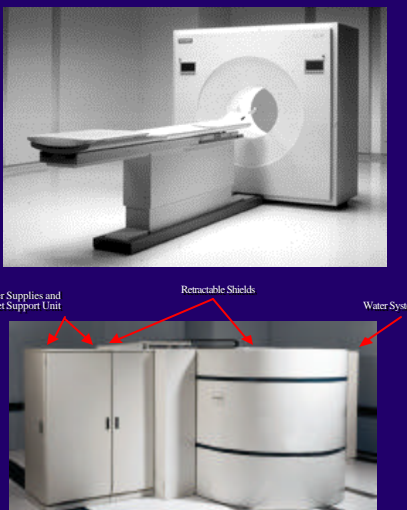
Photon Detection



3D PET Data Acquisition



Clinical PET systems



- Siemens CTI ECAT HR+ wholebody scanner.

~20,000 scintillator detectors (~32 rings x 576/ring)

ring diameter ~ 80 cm

4 mm (64 μ L) spatial resolution (typically 6-12 mm in clinical practice)

- CTI RDS 111 Cyclotron

MicroPET: Small Animal Imaging

- UCLA microPET system

~2,000 scintillator detectors (8 rings x 240/ring)

ring diameter ~ 17.2 cm

11.2cm x 1.8cm field of view

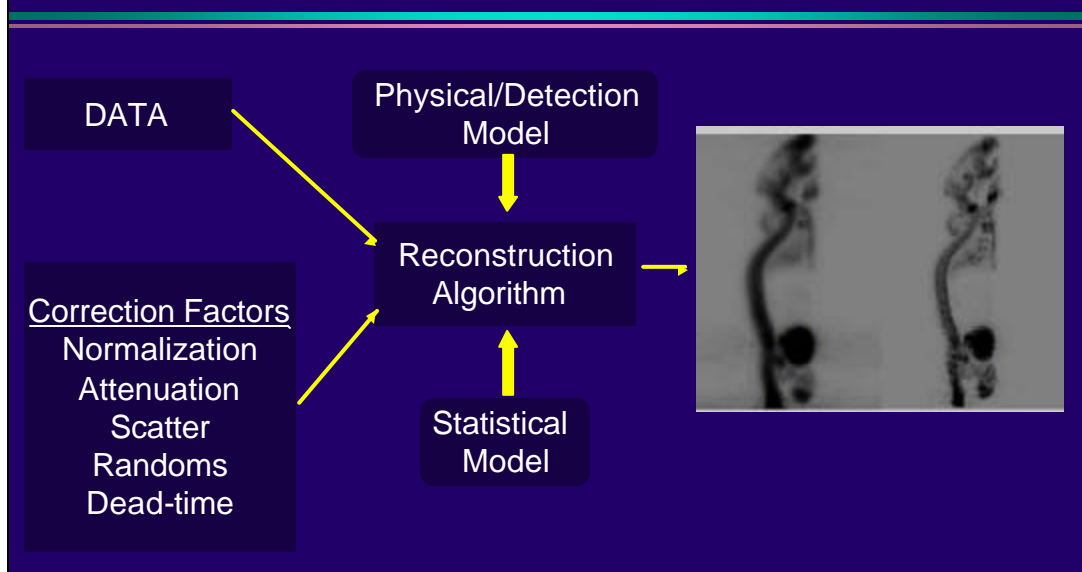
1.8 mm measured spatial resolution

Commercial version distributed by Concorde
microsystems for rodent (R4) and small primate
(P4) use.



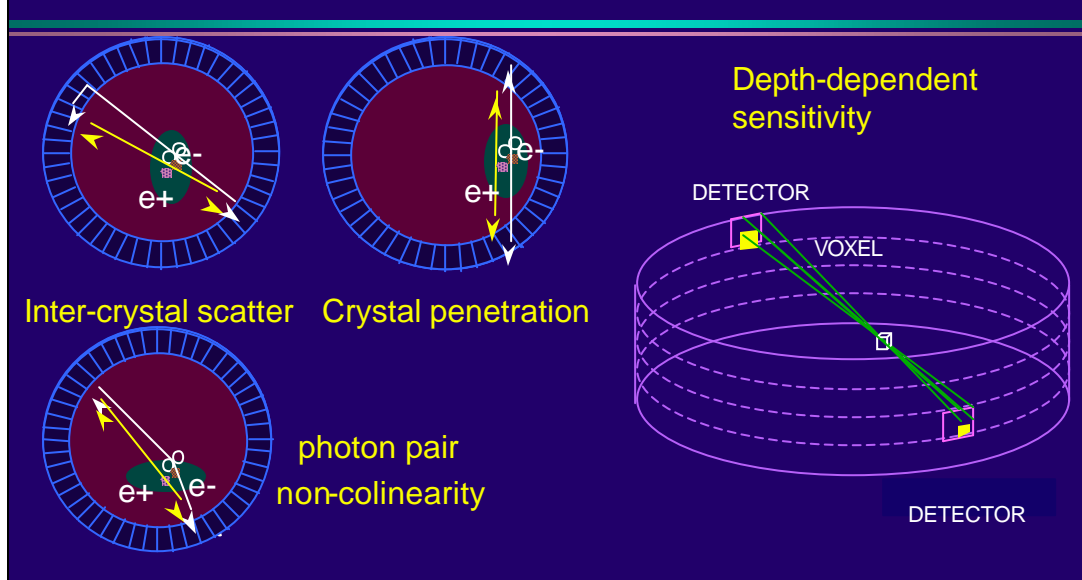
Model Based Image Reconstruction

Richard Leahy, USC, Dec 2002



Deviations from line-integral model

Richard Leahy, USC, Dec 2002



Physical and Statistical Models

$$\bar{\mathbf{y}} = \mathbf{P}\mathbf{x} \quad \mathbf{P} \in R^{10^7 * 10^6}$$

$$P = P_{Sens} P_{Blur} P_{Attn} P_{Geom} P_{range}$$

- P_{Range} : Positron range blurring matrix
- P_{Geom} : Geometric projection matrix
- P_{Attn} : Attenuation factor matrix (diagonal)
- P_{Blur} : Sinogram blurring kernel
- P_{sens} : Detectors sensitivity matrix (diagonal)

Data Models

- Data Model:

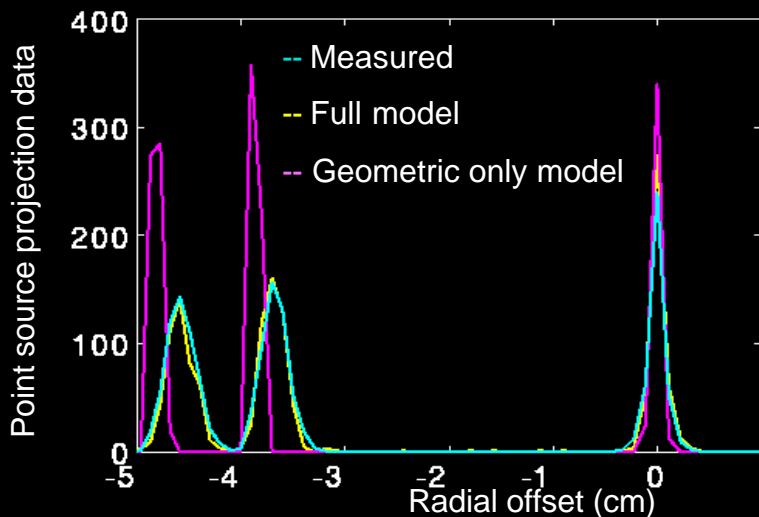
$$\bar{\mathbf{y}} = \mathbf{P}\mathbf{x} + \mathbf{r} + \mathbf{s}$$

- Poisson likelihood:

$$p(\mathbf{y}/\mathbf{x}) = \prod_i \frac{\bar{y}_i^{y_i} e^{-\bar{y}_i}}{y_i!}$$

- Modified Poisson model to account for subtraction of randoms from data (match 1st and 2nd moments).

Projection Profiles Comparison



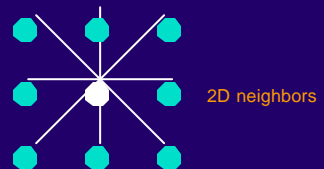
- 3 point sources with different radial offsets scanned in the microPET scanner.
- The projections were computed using forward model for comparison

MRF Image Priors

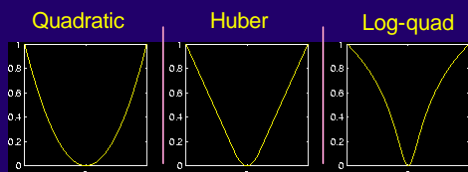
- Markov Random Field (MRF) with Gibbs distribution:

$$p(x) = \frac{1}{Z} \exp\{-\mathbf{b}U(x)\}$$

$$U(x) = \sum_i \sum_{j \in N_i, j > i} \mathbf{k}_{ij} V(x_i - x_j)$$



- Potential functions: $V(x)$



$$v(x) = x^2$$

$$\begin{cases} \frac{1}{2d}x^2, & \text{if } |x| \leq d \\ \left|\frac{x}{d}\right| - \frac{d}{2}, & \text{otherwise} \end{cases}$$

$$\log\left(1 + \frac{x^2}{d^2}\right)$$

Cost Functions

- Maximum likelihood:

$$\begin{aligned} x_{ML} &= \arg \max_x p(y | x) = \arg \max_x \{\ln p(y | x)\} \\ &= \sum_i y_i \log \bar{y}_i - \bar{y}_i \end{aligned}$$

- Maximum *a posteriori* (MAP) estimate:

$$x_{MAP} = \arg \max_x \frac{p(y|x)p(x)}{p(y)} = \arg \max_x \{\ln p(y|x) + \ln p(x)\}$$

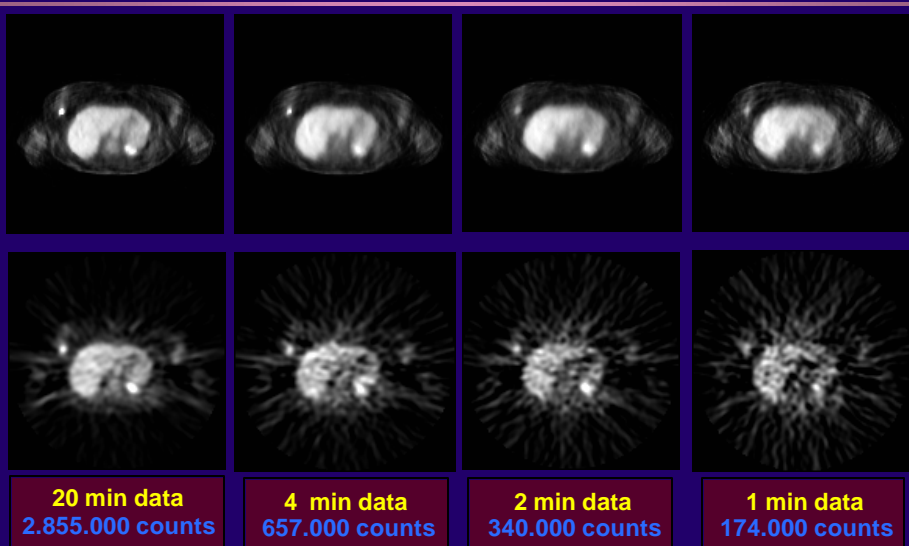
Smoothing Parameter Selection

- Estimation theoretic approaches:
 - » ML estimation: EM/MCMC, mean-field annealing
 - » Cross validation, L-curve
- Uniform smoothing parameters result in non-uniform resolution due to
 - » Non-uniform sensitivity and detector resolution
 - » Spatially variant noise
- use spatially-varying smoothing (see later).

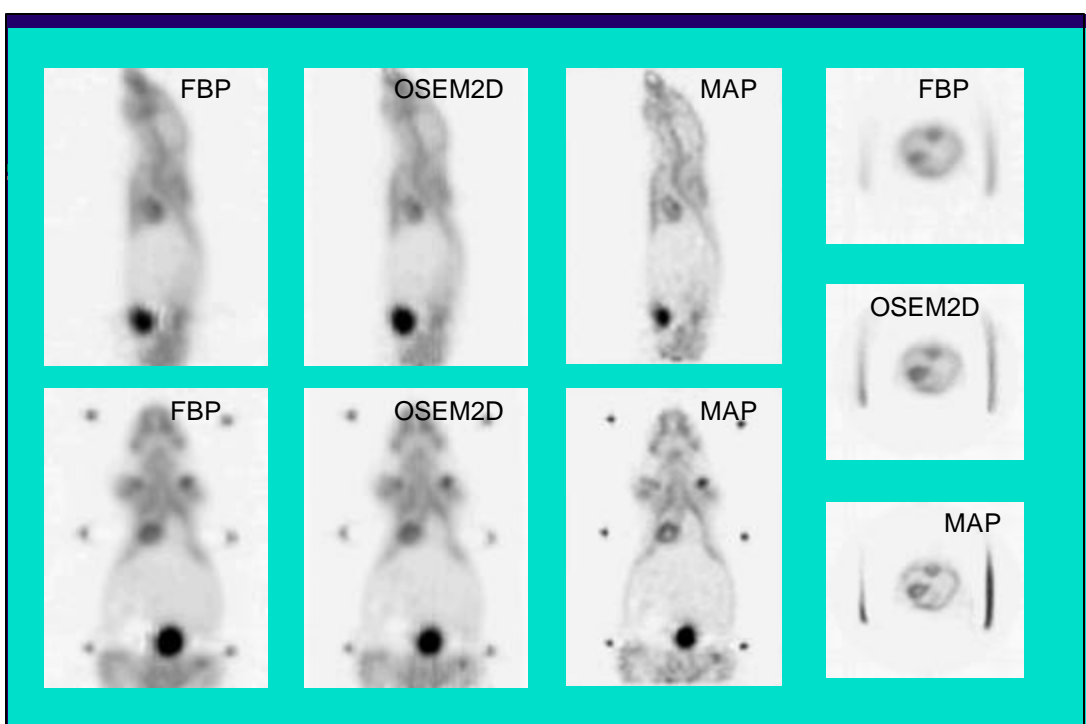
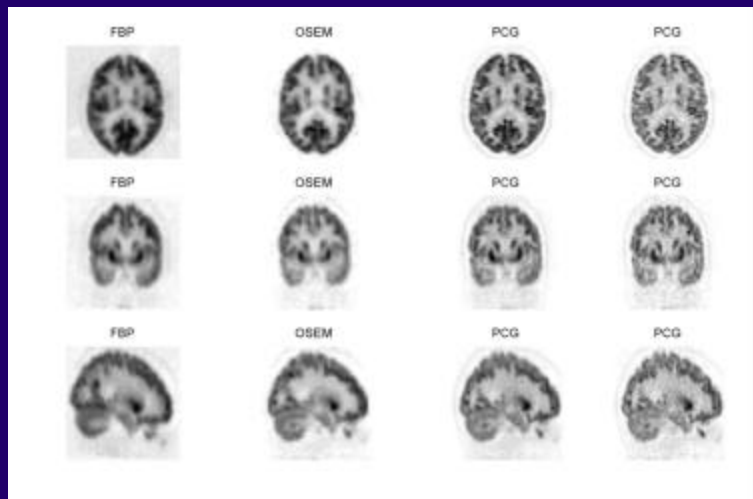
Reconstruction Algorithms

- **Filtered-Backprojection**
 - » Fully 3D with reprojection for “missing” data (Kinahan and Rogers)
 - » Fourier-rebinning + 2D FBP (Defrise et al)
- **Maximum likelihood**
 - » EM algorithm (Shepp, Vardi, Kaufman; Lange, Carson)
 - » OSEM and other block-iterative methods (Hudson, Larkin; Byrne)
 - » 2D OSEM – hybrid – Fourier rebinning and 2D OSEM (Comtat, Kinahan et al)'
 - » Seives (Snyder, Miller)
- **MAP**
 - » Generalized EM (Hebert, Leahy; Gindi, Lee, Rangarajan)
 - » Conjugate gradient methods (Kaufman, Qi, Leahy)
 - » Coordinate wise (Bouman, Sauer; Fessler)
 - » Functional substitution methods (dePierro; Fessler; Bouman, Sauer)
 - » Convergent, regularized “OSEM” (Ahn, Fessler).
 - » MAP with binary (edge) variables: ICA, mean field annealing or other continuation methods (Anand Rangarajan, Gindi, Lee, Rangarajan; Yan)

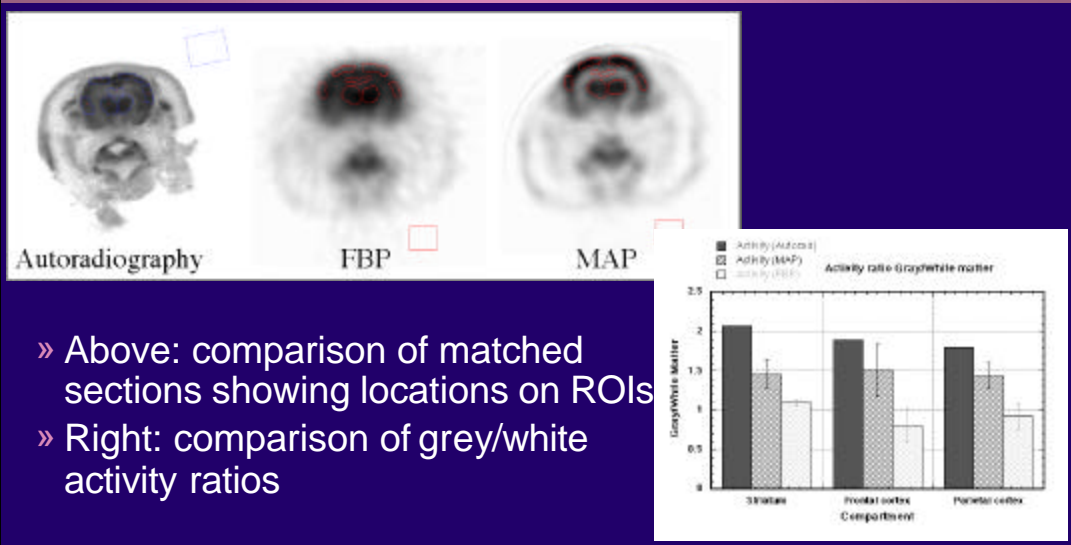
FDG Breast Cancer Study



Human FDG Scan



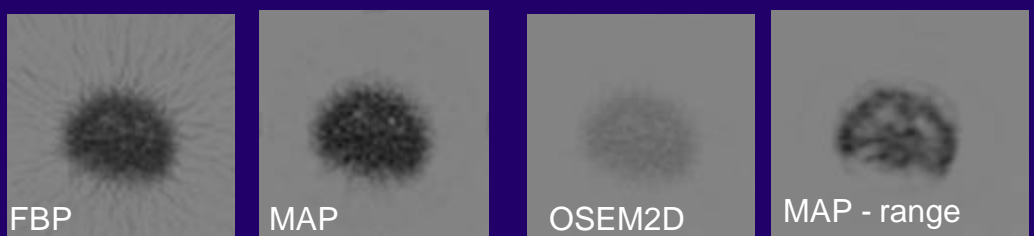
Autoradiography Study



- » Above: comparison of matched sections showing locations on ROIs
- » Right: comparison of grey/white activity ratios

Positron Range Compensation

- Model range as isotropic blurring of image using Monte Carlo distribution (R. Laforest, Wash. U)
- Cu-62 (2.93 MeV) baby monkey brain phantom, 20mins, 84M cts. (S. Cherry, UC Davis)



Attenuation Correction

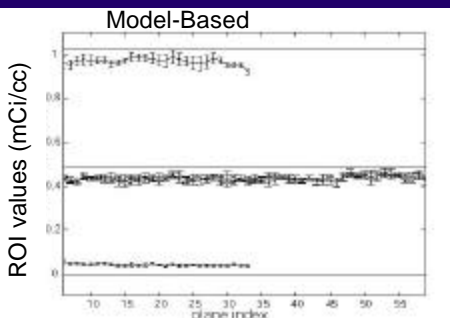
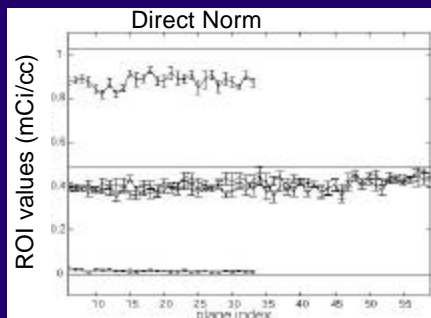
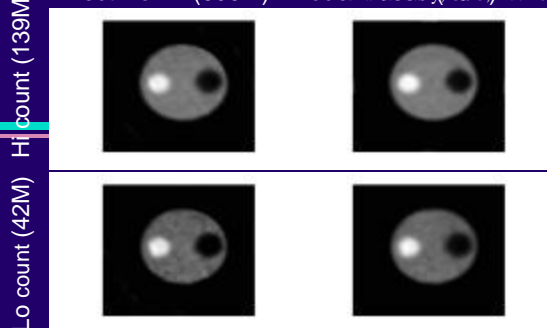
- MAP code readily adapted to transmission reconstruction from coincidence or singles data
 - » Cylinder phantom, 1 empty chamber
 - » Singles mode, 160 minutes blank and 160 minutes tx scan
 - » Voxel size 1mm



Normalization

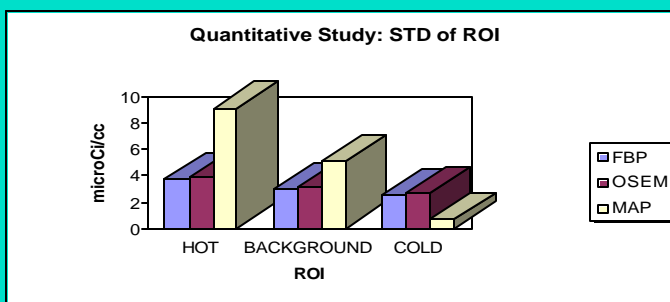
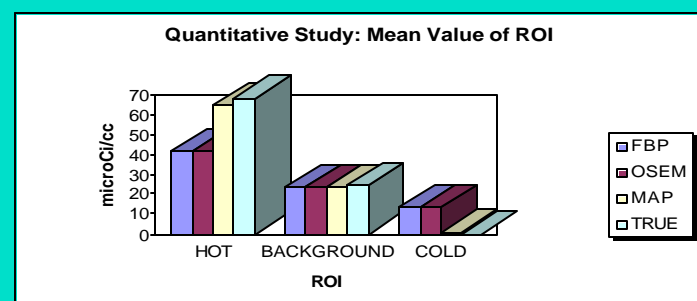
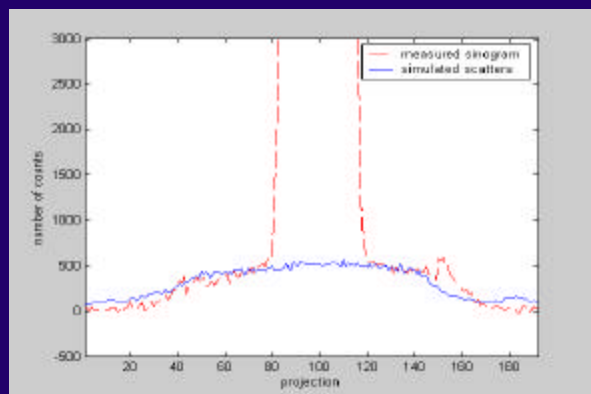
- Max likelihood norm estimation from cylinder scan:
 - » Geometric (block)
 - » Intrinsic
 - » Block timing
 - » Blockwise deadtime

Direct Norm (600M) Model-Based (70M) Dec 2002



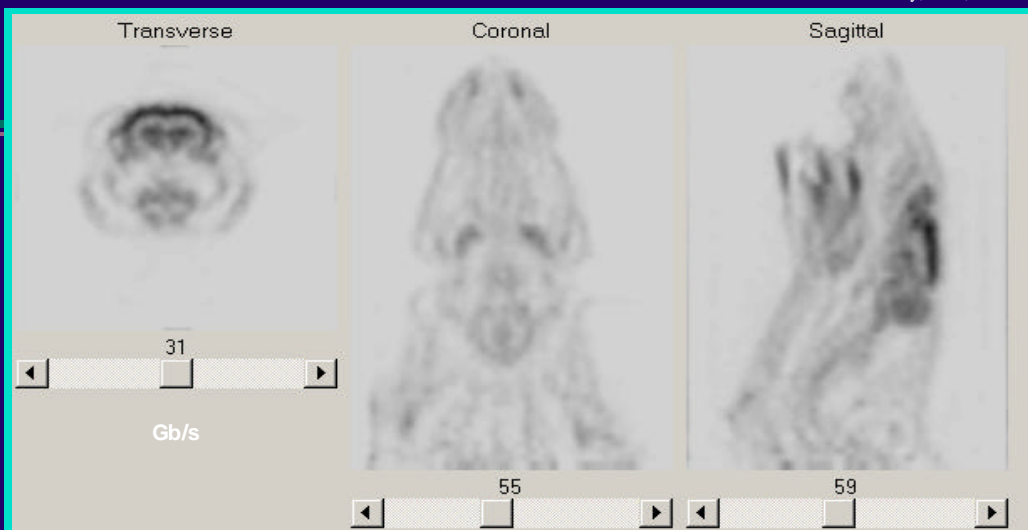
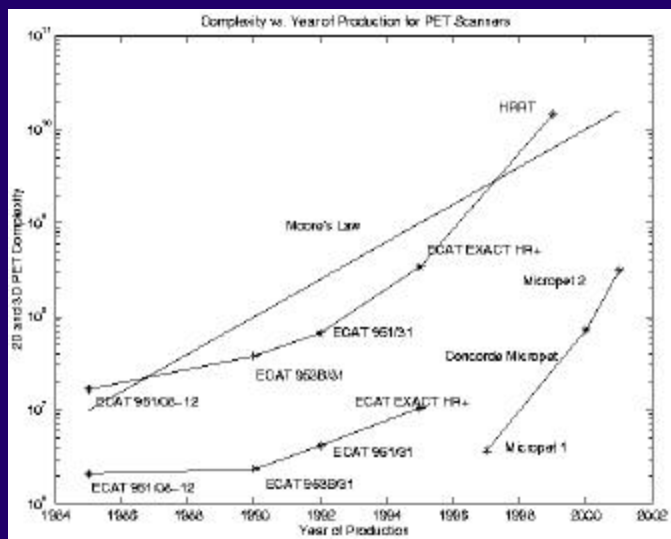
Scatter Correction

- Fast Monte Carlo based on attenuation and preliminary emission image -
 - Holdsworth C H, Levin C S, Janecek M, Dahlbom M and Hoffman E J 2002, Performance analysis of an improved 3D PET Monte Carlo simulation and scatter correction. IEEE Trans. Nucl. Sci. 48.



Computational Cost

- Reconstruction cost
 - » 2D PET: order $M^2 L N$ for M detectors per ring, L rings image reconstructed on planes of size N by N
 - » 3D PET order $M^2 L^2 N$ for M detectors per ring, L rings image reconstructed on planes of size N by N

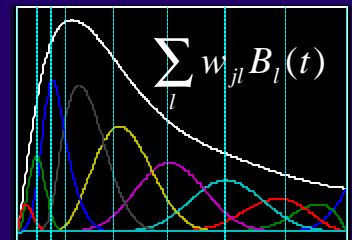


Processed in collaboration with Yasuyoshi Watanabe, Dept. Physiology, Osaka City University, Japan

Continuous time reconstruction: 4D PET

Richard Leahy, USC, Dec 2002

- Use list-mode data (arrival times of each detector pair) to compute estimate of continuous time PET image.
- Continuous-time function at each voxel
- Estimate set of spline control vertices for each voxel
- Uses spatial and temporal regularization
- Similar to list-mode reconstruction of Snyder(1984), Ollinger (1986) – used physiological basis functions.



4D PET

Richard Leahy, USC, Dec 2002

- Use list-mode data (arrival times of each detector pair) to compute estimate of continuous time PET image.

$$\mathbf{h}_j(t) = \sum_l \mathbf{w}_{jl} B_l(t)$$

$\mathbf{h}_j(t)$ = Activity at voxel j

\mathbf{w}_{jl} = Image of control vertices for each l

$B_l(t)$ = B-spline basis function

- Data:

$$\mathbf{I}_i(t) = \sum_j P_{ij} \sum_l \mathbf{w}_{jl} B_l(t) = \sum_l \left(\sum_j P_{ij} \mathbf{w}_{jl} \right) B_l(t)$$

Model: Poisson Process Likelihood

- For inhomogeneous Poisson process, arrival times $\{a_1, \dots, a_k, \dots, a_N\}$

$$p(a_1 \dots a_N | \mathbf{I}(t)) = \prod_{k=1}^N \mathbf{I}(a_k) e^{-\int \mathbf{I}(u) du}$$

- Log likelihood for imaging

$$L(D|W) = \sum_i \sum_k \log I_i^*(a_{ik}) - \sum_i \int I_i^*(u) du \quad I_i^*(t) \geq 0 \forall t$$

Where $I_i^*(t) = \sum_j \left(\sum_l P_{ij} w_{jl} \right) B_l(t) + r_i(t) + s_i(t)$

And a_{ik} is the arrival times of the k th count at the i th detector pair

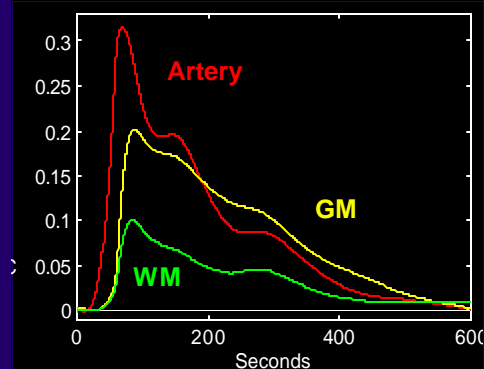
Estimation: Objective Function

$$L^*(W) = L(W) - \mathbf{ar}(W) - \mathbf{bf}(W) - \mathbf{gn}(W)$$

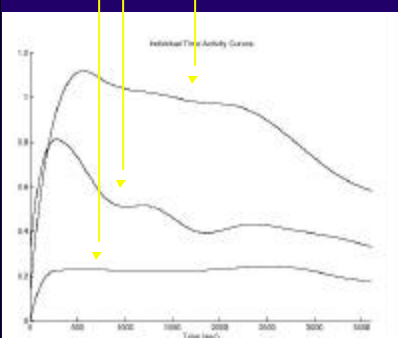
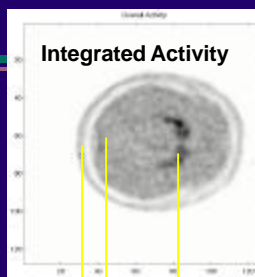
- Three penalty terms
 - $\mathbf{r}(W)$ Temporal Regularization
 - $\mathbf{f}(W)$ Spatial Regularization
 - $\mathbf{n}(W)$ Negativity Penalty
- Objective function negative definite

4D PET

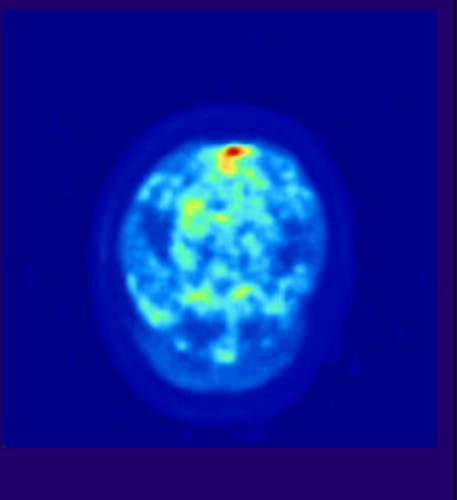
H_2^{15}O brain activation study, 3D HR+



C-11 Raclopride



^{11}C -Raclopride,
HR++,
Hammersmit
h, London.
90 min list
mode
acquisition,
fully 3D.



Performance Analysis

Experimental Evaluation

Quantitative accuracy

- FWHM resolution, noise variance
- ROI means and variances

Detection Performance

- Contrast recovery vs. variance
- Human observer ROC studies

Computational Evaluation

Monte Carlo studies

- bias, covariance, ROI accuracy
- human or machine ROC detection studies

Theoretical Performance Analysis

- Approximate expressions for bias, contrast recovery, covariance
- Analytical expression for ROC detection performance.

Taylor Series Approximation

$$\hat{x} = \arg \max_{\mathbf{x} \geq 0} \{ \ln p(y | x) - bU(x) \}$$

- First order Taylor series expansion of implicit estimator

$$\hat{x} = h(y) \approx h(\bar{y}) + \nabla h(\bar{y})(y - \bar{y})$$

- Use this expansion to approximate the local impulse response

$$l^j(\hat{x}) \approx \lim_{d \rightarrow 0} \frac{E[h(y(x + de^j))] - E[h(y(x))]}{d}$$

- and covariance of the MAP reconstruction.

Local Impulse Response and Covariance Approximation

Richard Leahy, USC, Dec 2002

- Local Impulse Response:

$$l^j(\hat{x}) \approx [F + bR]^{-1} Fe_j$$

- Covariance is approximated by

$$\begin{aligned} Cov(\hat{\mathbf{x}}) &\approx \nabla h(\bar{y}) Cov(y) \nabla h(\bar{y})' \\ &\approx [F + b R]^{-1} F [F + b R]^{-1} \end{aligned}$$

Where F is the Fisher information matrix:

$$F_{M \times M} \equiv P \text{ diag}[\bar{y}_i^{-1}] P$$

R is the second derivative of prior energy function $U(x)$.

Richard Leahy, USC, Dec 2002

Approximation Results (i)

- Simplified Fourier-transform based expressions for local impulse response and covariance (assuming shift invariant response of GG^T , where $P = \text{diag}(.)G$):

$$crc_j \approx \frac{1}{N} \sum_{i=0}^{N-1} \frac{I_i(j)}{I_i(j) + b k_j^{-2} m_i(j)}$$

$$Cov_j(\hat{\mathbf{x}}) \approx k_j^{-2} Q^T \text{diag} \left[\frac{I_i}{(I_i + b k_j^{-2} m_i)^2} \right] Q e^j$$

where

$$G^T G = Q^T \text{diag}[I_i] Q, \quad R = Q^T \text{diag}[m_i] Q,$$

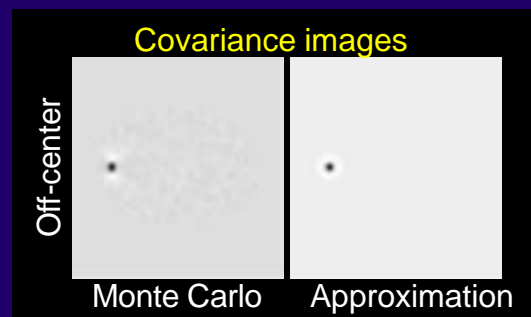
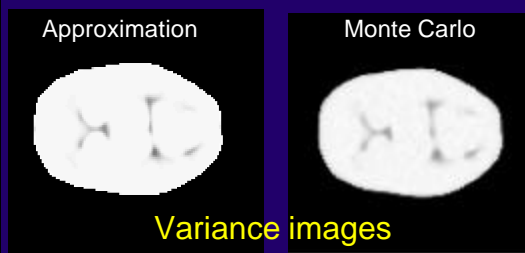
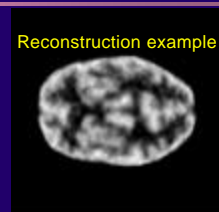
$$k_j^2 = f_{jj} = \sum_i g_{ij}^2 n_i^2 / \bar{y}_i$$

Applications

- Algorithm and system comparison (contrast and noise properties)
- Selection of β to maximize detection through maximization of contrast to noise ratio
- Estimation of ROI variances
- Selection of spatially variant β for uniform resolution
- Quantifying ROC detection performance for computer observers

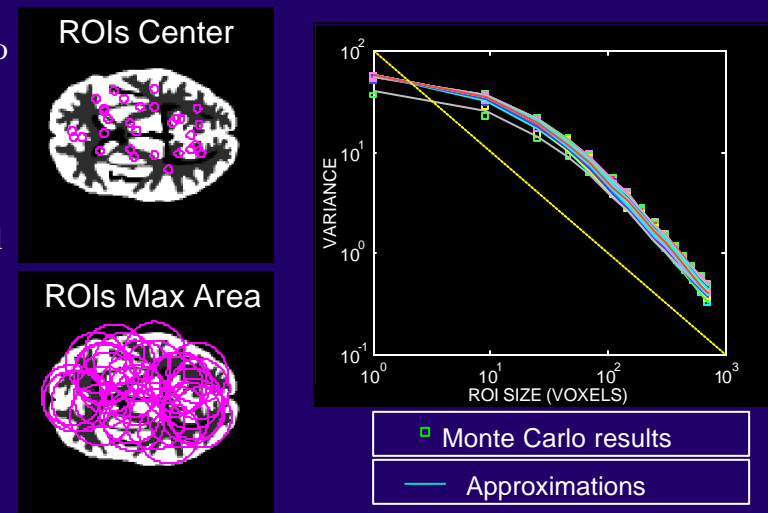
Covariance Approximation

Simulated 2D mode of CTI ECAT HR+ PET scanner using Hoffman brain phantom with GM:WM:CSF=5:1:0. Uniform attenuation. Total counts = 200,000. 8,000 Monte Carlo data sets were reconstructed.



Approximation of ROI variance

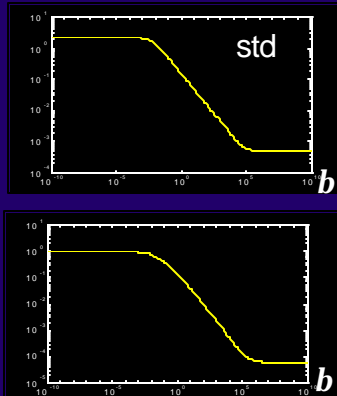
- 8000 Monte Carlo reconstructions use to find variance of each ROI.
- Each data set has approximately total counts of 200k



Maximizing lesion detectability

Choose smoothing parameter to maximize contrast to noise ratio.

$$\mathbf{b}_j = \arg \max_{\mathbf{b}} \frac{crc_j}{\sqrt{\text{var}_j}}$$



Maximizing lesion detectability (ii)

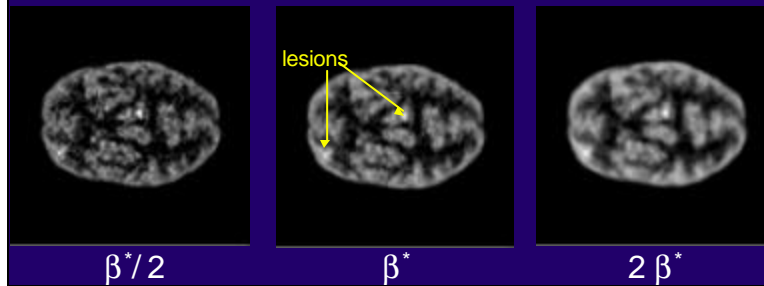
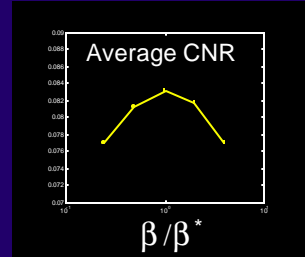
Richard Leahy, USC, Dec 2002

computer generated independent data sets

Total count 200k

Each data set was reconstructed with β^* and $\beta^*/4, \beta^*/2, 2\beta^*, 4\beta^*$.

The variance



Richard Leahy, USC, Dec 2002

Spatially Variant Smoothing Prior

- To get uniform resolution, we proposed a spatially variant smoothing prior of which the energy function is:

$$U(x) = \frac{1}{2} \sum_i \sum_{j \in N_i, j > i} \sqrt{\mathbf{b}_i \mathbf{b}_j} \mathbf{r}_{ij} (x_i - x_j)^2$$

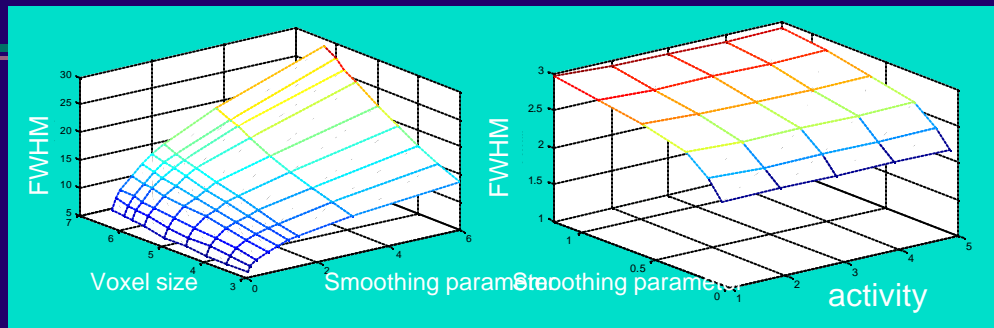
- The second derivative at voxel j is

$$\begin{aligned} & -\frac{1}{\sqrt{2}} \sqrt{\mathbf{b}_{i_0} \mathbf{b}_j} \quad -\sqrt{\mathbf{b}_{i_1} \mathbf{b}_j} \quad -\frac{1}{\sqrt{2}} \sqrt{\mathbf{b}_{i_2} \mathbf{b}_j} \\ & -\sqrt{\mathbf{b}_{i_3} \mathbf{b}_j} \quad \underbrace{-\sum_{i \in N_j} \sqrt{\mathbf{b}_i \mathbf{b}_j} \mathbf{r}_{ij}}_{|} \quad -\sqrt{\mathbf{b}_{i_5} \mathbf{b}_j} \quad \text{2nd order} \\ & -\frac{1}{\sqrt{2}} \sqrt{\mathbf{b}_{i_6} \mathbf{b}_j} \quad -\sqrt{\mathbf{b}_{i_7} \mathbf{b}_j} \quad -\frac{1}{\sqrt{2}} \sqrt{\mathbf{b}_{i_8} \mathbf{b}_j} \end{aligned}$$

- An iterative procedure is needed to find the appropriate \mathbf{b} 's for the desired resolution CRC* because $\mathbf{m}(j)$ is dependent on \mathbf{b} . We solve an approximate system for the \mathbf{b} 's.

$$crc^* \approx \frac{1}{N} \sum_{i=0}^{N-1} \frac{\mathbf{I}_i(j)}{\mathbf{I}_i(j) + \mathbf{b} \mathbf{k}^{-2} \mathbf{m}_i(j)}$$

Uniform Resolution



- Through spatially adaptive smoothing:
 - » Spatially invariant resolution
 - » Beta vs. resolution monotonic
 - » Resolution independent of activity

Thanks

- **Collaborators**
 - » **UC Davis**: Simon Cherry, Craig Abbey
 - » **UCLA**: Arion Chatzioannou, Fernando Rannou, David Stout, Magnus Dahlbom, Mike Phelps
 - » **Lawrence Berkeley**: Jinyi Qi, Ron Huesman
 - » **Washington University**: Richard Laforest, Y.C. Tai
- **Concorde microSystems, CTI, Knoxville**
- **NIH support**: National Institute for Biomedical Imaging and Bioengineering
- **USC** - *Bing Bai, Evren Asma, Quanzheng Li, David Shattuck, Peter Conti, Jim Bading*
- **Ongoing Software Evaluation**
 - » **BNL**: Wynne Schiffer, Joanna Fowler
 - » **Max Planck Inst, Koln**: Klaus Wienhard, Stefan Vollmar Christof Knoess.
 - » **Osaka City Univ**: Yasuyoshi Watanabe
 - » **Univ Michigan, Ann Arbor**: Robert Koeppe
 - » **National Tsing-Hua Univ, Taiwan**: Ching-Han Hsu